Surface chemistry and flotation properties of galena and pyrite particles in the presence of xanthate- monothiophosphate- thiocarbamate collectors

Gokhan Ercelik [1], Mert Terzi [1], Ilgin Kursun [1], Orhan Ozdemir [2]

[1] Istanbul University-Cerrahpasa, Department of Mining Engineering, Buyukcekmece, Istanbul, Turkey

[2] Istanbul Technical University, Department of Mineral Processing Engineering, Maslak, Istanbul, Turkey

Corresponding authors: ilginkur@iuc.edu.tr, orhanozdemir@itu.edu.tr (Ilgin Kursun, Orhan Ozdemir)

Abstract: In this study, surface chemistry and flotation properties of the gold-bearing galena and pyrite minerals of Menderes region, Izmir, Turkey were investigated with the use of xanthate-thiocarbamate-monothiophosphate collectors. In this context, the micro-flotation experiments, the zeta potential, and bubble-particle attachment time measurements were conducted in the presence of Thiophosphate (Aero S-8045), Xanthate (SIBX), and Thiocarbamate (Aero float MX-505) collectors. In the case of micro-flotation experiments, the MX-505 exhibited higher flotation efficiency for both minerals compared to SIBX and S-8045 collectors. In the micro-flotation tests conducted on galena and pyrite, while the flotation recovery of 99.82% and 81.96% were obtained with MX-505, the flotation recovery of 89.64% and 62.50% were reached in the case of using SIBX. Furthermore, the S-8045 resulted in the flotation recovery s of 75.09% and 25.45% for galena and pyrite, respectively. In the case of zeta potential experiments as a function of pH, the galena mineral showed a negative charge between -17.22 to -41.42 mV at pH 5 – 11, no point of zero charge (pzc) was determined, and the pzc of pyrite was determined as pH≈8. The bubble-particle attachment time experiments performed in the presence of S-8045, SIBX, and MX-505 collectors indicated that the attachment efficiency was 100% in the presence of MX-505 at 12.5-75 g/Mg dosages and 1-1000 ms contact times. These results revealed that there was an extraordinarily strong interaction between the galena/pyrite and the air bubbles in the presence of MX-505. The results obtained within this study indicated that galena and pyrite minerals showed inherently less than 25% natural floatability which can only be enhanced under specific conditions. The results obtained within this study indicated that galena and pyrite minerals showed inherently low natural floatability which can only be enhanced under specific conditions. In the tests conducted on these minerals, galena mineral showed higher than %20 natural floatability compared to pyrite mineral, and collectors produced from thiocarbamates have shown greater effectiveness compared to xanthate and thiophosphate.

Keywords: pyrite, galena, zeta potential, bubble-particle attachment time, micro-flotation

1. Introduction

The prospecting and enrichment of metallic ores are carried out through comprehensive processes. Mineralogy and metallurgical properties of any given ore determine the enrichment process to be applied, as well as influence the commercial value of the product obtained depending on the efficiency of the operation. In one of the enrichment methods, froth flotation, it is necessary to have a good knowledge of the mineralogy and surface chemistry of the ore to obtain high performance (Delany, 1940; McKee, 1991; Hodouin et al., 2001). Although many studies have been carried out on the surface chemistry and flotation aspects of pyrite and galena (Gaudin & Malozemoff, 1932; Finkelstein & Poling 1977; Kocabag, 1983; Kocabag et al., 1990; Elizondo et al., 2017), detailed experimental studies are still required, especially for the different ores specific to deposit because, depending on the characteristics

of the deposit and the formation modes, minerals can show different properties and behaviors. Also, the chemicals used for covering the mineral surface impact surface chemistry.

Xanthate chemical is commonly used in sulfide ores containing pyrite and galena. However, due to factors such as performance, selectivity, synergistic effect, etc., the usage of thiocarbamate and blend chemicals is becoming more widespread (Nagaraj and Ravishankar, 2007). An increase in dosage in the singular use of xanthate collector will result in concentration at the previously attached points on the mineral surface, while not affecting other areas of the mineral surface. Therefore, in this case, the use of blend types of dithiophosphate and thiocarbamate chemicals will be more effective in coating the entire chemical surface (McFadzean, 2013). As an active topic in flotation literature since the 1930s (Swainson and Anderson, 1931; Herd and Ure, 1941; Gaudin et al., 1942) investigation on the flotation properties and surface interactions on galena and pyrite-xanthate systems in the presence of different xanthate compounds were continued in several recent studies (Elizondo et al., 2018; Özün and Ergen, 2019; Cui et al., 2021). Many of these studies have been focused on the selective separation of galena and pyrite from other sulfides or gangue minerals and the obtained results have supported the fundamentals of galena/pyrite-xanthate interaction and confirmed the effectiveness of xanthates in both galena and pyrite flotation systems.

Studies have also been conducted on thiophosphate and thiocarbamate chemicals, but compared to other investigations, there are fewer comprehensive studies on blend chemicals in the literature. Experimental studies on non-blend chemicals have found that the performance of thiocarbamate chemicals is superior to xanthate. On the other hand, thiophosphate has been found to act as an auxiliary collector to xanthate, resulting in lower performance (Shen et al., 2016).

In many of the studies focused on xanthate, thiophosphate, and thiocarbamate collectors, several methods such as zeta potential, adsorption density, and contact angle measurements (McFadzean, 2013; Zhang et al., 2019; Huang et al., 2019) have been realized in parallel with surface-based analysis methods such as XPS, FTIR, AFM, and TOF-SIMS (Owasu et al., 2014; Long et al., 2016; Jin et. al., 2020; Chen et al., 2021; Dong et al., 2021). Another parameter that can be used to assess the flotation performance is the particle-bubble interaction, which its use has been limited compared to the previously mentioned methods (Nikolaev et al., 2019; Qi, et al., 2020).

The efficiency of the flotation process is dependent on the behaviour of hydrophobic mineral particles that are collected by air bubbles. Generally, the flotation properties of a mineral are determined by contact angle measurements. However, the results obtained in several studies have shown that this method is not always able to accurately predict the flotation property of a mineral (Ye & Miller, 1988; Yoon & Yordan 1991). Another method for predicting the floatability of a mineral is the determination of the bubble-particle attachment time, which is determined by measuring the time required for the particle to adhere to the air bubble. Bubble-particle attachment time determination measurements provide a more accurate approach than contact angle in determining the flotation behaviour of the mineral (Ye & Miller, 1988; Gu et al., 2003; Su et al., 2006; Ozdemir et al., 2009; Albijanic et al., 2011, 2014). In addition, the analysis of zeta potential measurements is essential for gaining a comprehensive understanding of both the electrokinetic properties of particles and the flotation separation process (Nguyen, 1994).

In this study, zeta potential and bubble-particle attachment time measurements and micro-flotation experiments were conducted on gold-bearing galena and pyrite minerals originating from Izmir province, Turkey. Moreover, the effects of Aerofloat MX-505 and Aero S-8045, which are collector blends that are respectively based on thiocarbamates and thiophosphates, on pyrite and galena were investigated to correlate zeta potential and bubble-particle attachment time measurements, and micro-flotation results, first time in the literature.

2. Materials and methods

2.1. Materials

The galena and pyrite-rich coarse ore particles were representatively taken from the feed of a gold processing plant of a private company in the Izmir-Menderes region, Turkey. After the crushing and classification steps, pure galena and pyrite minerals were obtained by employing hand sorting under an optic microscope. Pure pyrite and galena minerals used in the experiments are shown in Fig. 1.

The results of the mineral phase analysis carried out by X-ray diffraction (XRD) on pure samples are shown in Fig. 2. Characteristic peaks for both the galena and pyrite samples indicate that they were of high purity. The results indicated that the purity of both samples was found to be approximately>98% (± 2% equip. fudge factor). The collectors used in this study are also presented in Table 1.
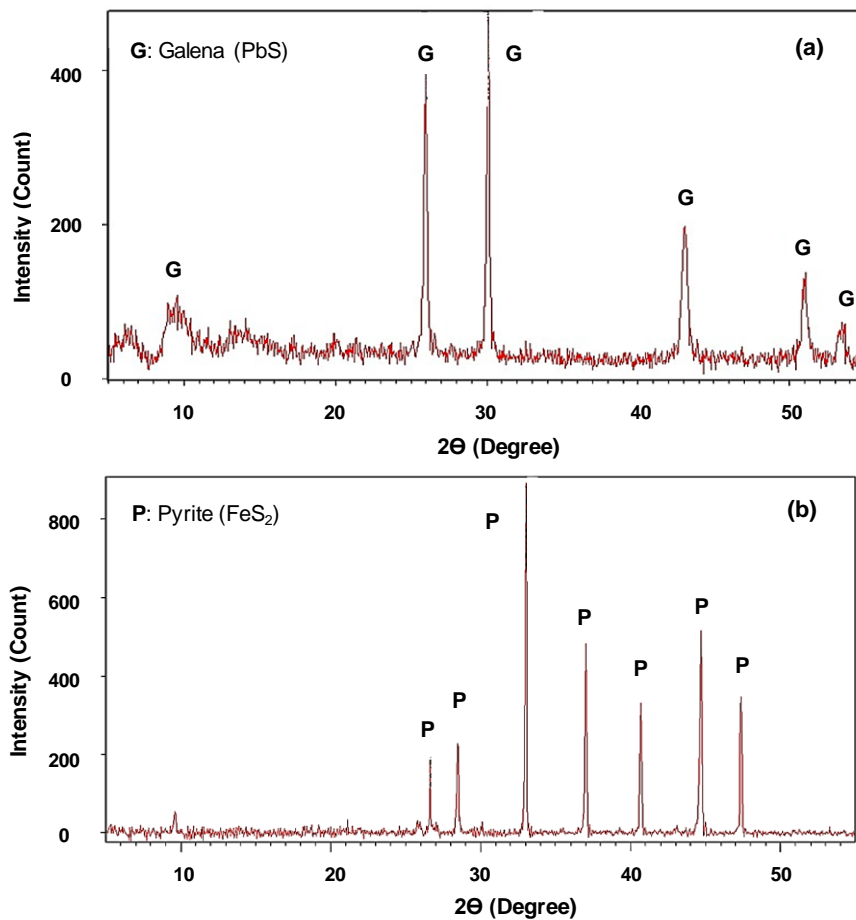

Fig. 1. Pure pyrite(a) and galena(b) samples

Fig. 2. X-ray diffraction patterns of (a) galena and (b) pyrite minerals

2.2. Methods

2.2.1. Micro-flotation experiments

A Partridge and Smith cell with a 55 cm³ volume was used in micro-flotation experiments (Partridge & Smith, 1971). The micro-flotation experiments were conducted with pure samples of 63×38 µm particle size to simulate plant conditions. The solids ratio of the suspension was selected as 1%. Three different collector types, namely xanthate, monothiophosphate, and thiocarbamate, were used in the experiments. The experimental parameters and chemicals used in this study are presented in Table 2.
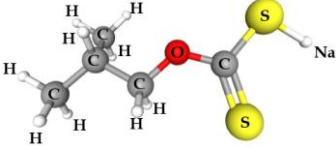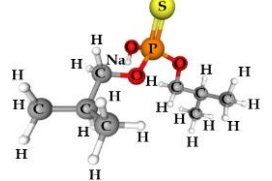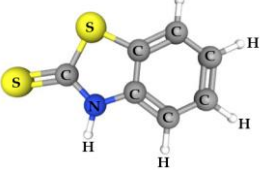
Table 1. Chemical properties and structures
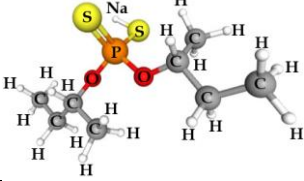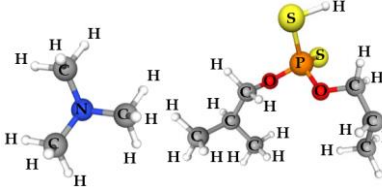
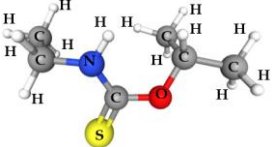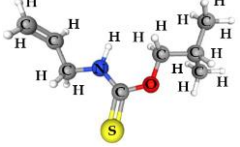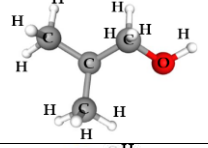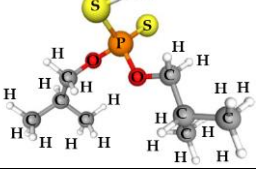| Name	Chemical Formula	Quantity	Chemical Composition and Formula
SIBX RC320 (Xanthate) (Quimidroga)		>95%	Sodium isobutyl xanthate $C_5H_9NaOS_2$
Aero S-8045 (Thiophosphate) (Solvay)		>40%	Sodium diisobutyl monothiophosphate $C_8H_{18}NaO_3PS$
		>30%	Sodium mercaptobenzothiazole $NaC_7H_4NS_2$
		10%	Sodium diisobutyl dithiophosphate $C_8H_{18}NaO_2PS_2$
		5%	Sodium di sec butyl dithiophosphate $C_8H_{18}NaO_2PS_2$
Aerofloat MX-505 (Thiocarbamate) (Solvay)		45%	Phosphorodithioic acid, O, O-bis(2-methylpropyl) ester, compound with- N, N dimethylmethanamine $C_{11}H_{28}NO_2PS_2$
		25%	Isopropyl ethyl thionocarbamate $C_6H_{13}NOS$
		25%	N-Allyl-O-isobutyl thionocarbamate $C_8H_{15}NOS$
		4%	2-Metilpropan-1- $C_4H_{10}O$
		1%	Diisobutyl- dithiophosphoric acid $C_8H_{19}O_2PS_2$

Table 2. Parameters and conditions for the micro-flotation experiments

Parameters	Conditions
Cell volume	55 cm^3
Water	Pure water (TDS<10/pH $\approx$ 7)
Sample amount	0.55 g
Particle size	63×38 μm
Solids ratio	1%
Stirring	500 rpm
Air Flowrate (N$_2$)	15 cm^3/min
pH	pH 8.7
Collector 1	SIBX (Quimidroga)
Collector 2	Aero S-8045 (Solvay)
Collector 3	Aerofloat MX-505 (Solvay)
Conditioning	8 min
Flotation time	1 min

2.2.2. Zeta potential measurements

The zeta potential measurements for the particles were conducted by electrophoretic method with a zeta meter (Zeta Plus, Brookhaven Instrument Ltd., USA). In this scope, first, a 0.3 g sample of galena with a size of -10 μm was mixed with 30 cm^3 of pure water (TDS<10 and pH $\approx$ 7) at 1% solids ratio using a magnetic stirrer at 500 rpm for 5 min. The pH of the suspension was adjusted with 0.1 mol/dm^3 HCl for an acidic medium or 0.1 mol/dm^3 NaOH solution for a basic medium. After the mixing process, the suspension was kept for 5 min to allow the coarse particles to settle down. Approximately 3 cm^3 aliquots were drawn from the surface of the suspension and transferred to the measurement cell with a 4 cm^3 volume. Finally, the measurements were carried out at different pH values (5-11). The average value for 20 measurements was calculated for each pH value. All zeta potential measurements were performed at 23°C temperature.

2.2.3. Bubble-particle attachment time experiments

Bubble-particle attachment experiments are conducted before conventional flotation gives critical information about the interaction between mineral-bubble, the floatability of the mineral (Nguyen and Schulze, 2004), interpretation of the flotation kinetics (Albijanic, et al., 2010; Xing et al., 2017), and the mechanism between chemicals and minerals. Although there are many studies on sulfide minerals (Gaudin et al. 1957; Glembotsky et al. 1963), each sample can show different properties due to its closed minerals formula, geomorphologies, and chemical decompositions.

In this study, the bubble-particle attachment time was determined with the BKT-100 bubble-particle attachment time device (Bratton Engineering and Technical Associates, LLC, USA). The related experimental setup is shown in Fig. 1. The bubble-particle attachment time experiments were conducted at different dosages of S-8045, SIBX, and MX-505 collectors A device with Glembotsky design concept (Bratton Engineering) was used to determine the particle-bubble attachment time (Glembotsky, 1953). In the experiments, the 0.5 g of 63×38 μm galena sample was conditioned with a collector solution of 50 cm^3 for 5 min by a magnetic stirrer at 500 rpm. Then, the measurement cuvette was filled with this suspension and hence a particle bed was formed on the floor of the cuvette. About 2 mm of air bubble was used for the bubble-particle attachment time experiments. For the particle-bubble attachment time measurements, the contact times of 1 ms, 10 ms, 100 ms, and 1000 ms were chosen. Ten different measurements were taken from the particle bed surface for each contact time. This procedure was performed 20 times at various places in the particle bed, and the results were recorded. And, the bubble-

particle attachment time was calculated as the time for which 50% of the observations resulted in an attachment. More details on the experimental procedure are given in another study (Ozdemir et al., 2006; Ozdemir et al., 2009; Güngören et al., 2019).

3.   Results and discussion

3.1. Micro-flotation experiments

Galena sample demonstrated a natural floatability (~%20) to a degree without a collector at natural pH. This recovery rate is also in parallel with the values obtained in the previous studies (McFadzean et al., 2012). Galena flotation is usually realized at mild alkaline conditions in practice and the pH ranges of 8.5-9.0 have been used in several studies accordingly (Bulatovic, 2007; Ikumapayi et al., 2012; Chen et al., 2021). However, the pyrite sample does not show any floatability at natural pH (pH 5). The results of microflotation experiments conducted with SIBX at different pH values are shown in Fig. 3.
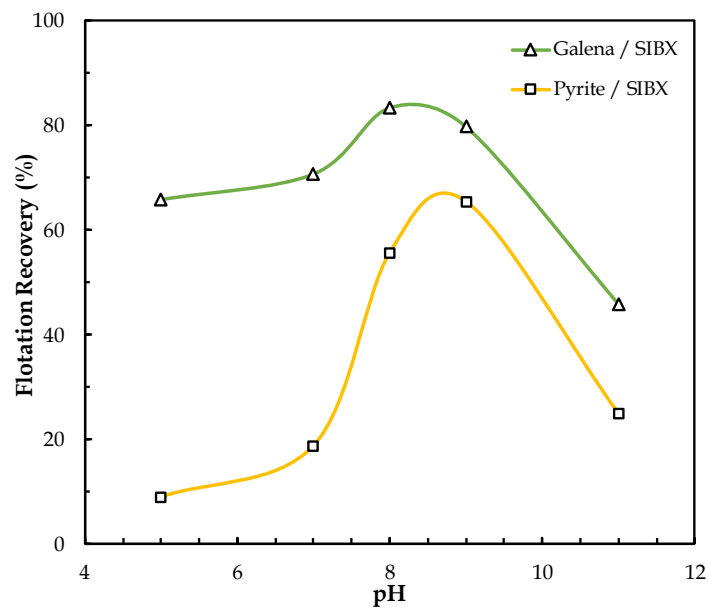

Fig. 3. Results for the micro-flotation experiments of pyrite and galena particles as a function of pH in the presence of 50 g/Mg SIBX

As seen in Fig. 3, the flotation recovery of galena was higher than that of pyrite at all pH conditions, and the highest recoveries were obtained between pH 8.5 to 9 for each of the minerals. Moreover, a significant decrease in the flotation recovery for both galena minerals was observed in the acidic and alkaline conditions. In acidic and neutral pH conditions, the pyrite flotation recovery was very low. The recovery of pyrite also decreased after pH 9. Similar recovery values at strong alkaline conditions in the flotation of pyrite with SIBX have also been reported by Huang et al. (2023) which can be attributed to the weakening of the adsorption of the collector on the pyrite surface due to the overlayer under strong alkaline conditions (Fairthorne et al., 1997). Accordingly, the optimum flotation pH values for both minerals were determined as 8.7, which is also the natural pH of the ore that the pure samples originated.

Fig. 4 shows the effect of collector dosage on the flotation behaviour of galena and pyrite minerals. Evaluating the results shown in Fig. 4, it can be observed that S-8045 was ineffective on pyrite, and only a 25% recovery was achieved at the highest collector dosage. Furthermore, the use of S-8045 also resulted in the lowest recovery of galena at the highest dosage. During the experiments conducted with the SIBX collector, an increase in the flotation recovery was observed in direct correlation with the dosage increment. The highest recovery achieved was 63% for pyrite and 90% for galena.

The highest pyrite and galena recoveries were obtained with MX-505 at 75 g/Mg dosage during these tests. At this dosage level, the recovery was reached to 82% for the pyrite mineral, and to 100% for the galena mineral. In these tests, it was observed that MX-505 positively changed the froth structure.

The alcohol-based components and surface activity in the structure of MX-505 led to an increase in the size and quantity of froth.

Additionally, all flotation performances increased with the increased collector dosages. The highest recovery values were reached with SIBX and MX-505. However, it can be said that better results were achieved by the usage of MX-505 compared to SIBX.

S-8045 collector did not provide promising results in terms of the flotation performance in singular use. The performance order of the collectors on pyrite and galena minerals was found to be MX-505 > SIBX > S-8045 (Somasundaran & Nagaraj, 1984; Nagaraj, 1988).
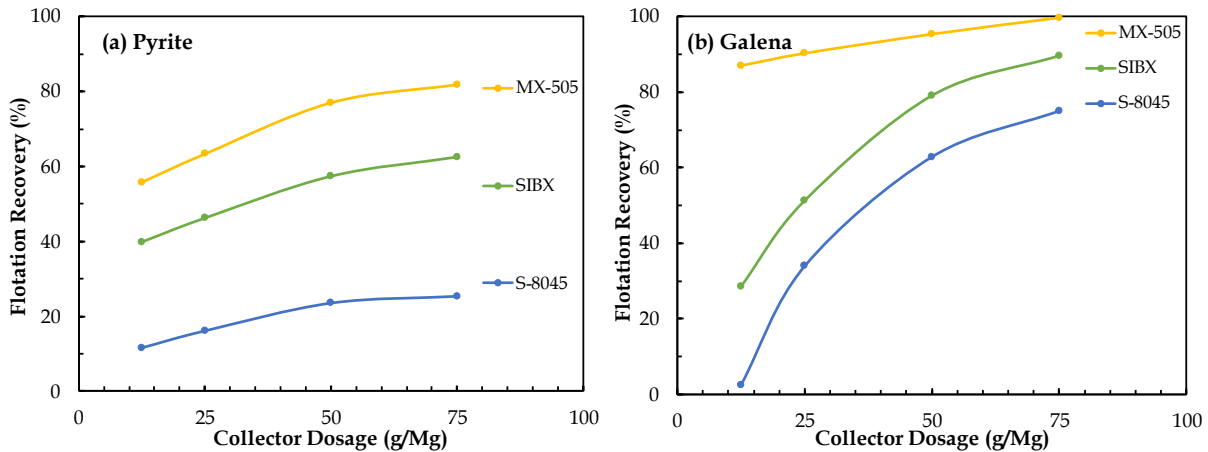

Fig. 4. Results for the micro-flotation experiments of pyrite and galena particles at natural pH as a function of collector dosages

3.2. Zeta potential measurements

The zeta potential measurements for the galena and pyrite samples were carried out as a function of pH, and the results are shown in Fig. 5. As seen from Fig. 5, the galena sample showed a negative surface charge for the values between 5-11, and the negativity decreased with the decreasing pH, and no point of zero charge (pzc) for the galena sample was determined under the experimental conditions. But, as known from the literature, different pzc values were determined for the galena minerals from 3 to 7.7 (Jiang et al., 1998; Pecina et al., 2003; Vilinska et al., 2007; Kosmulski, 2009; Bae et al., 2012; Consuegra, et al., 2020; Jin et al., 2021).

Flotation chemicals mainly adsorb at the mineral/solution interface and affect the surface properties of the mineral (Feng et al., 2019; Zhao et al., 2019). The zeta potentials of galena and pyrite minerals were measured between pH 5 to 11 in the presence of four different dosages from 12.5 g/Mg to 75 g/Mg
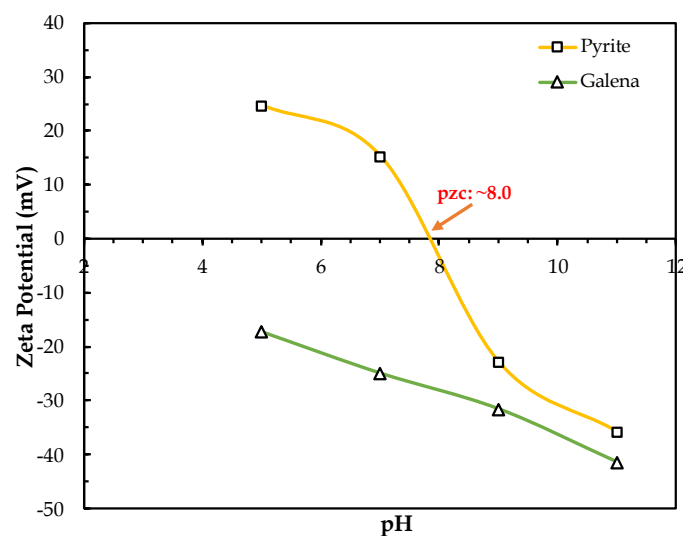

Fig. 5. Results for zeta potential measurement of galena and pyrite minerals as a function of pH

with three type collectors (Figs. 6 and 7).

Interaction between SIBX and pyrite/galena surface indicates that SIBX could adsorb on its surface. The increase in the zeta potential of pyrite/galena (especially pH=9) at elevated dosages of SIBX was higher compared to the values obtained at lower dosages, which indicates a strong interaction between SIBX and pyrite/galena (Fig. 6). Adsorption of cations in the solution leads to an increase in the zeta potential in the negative direction. This can be explained by the replacement of positively charged different iron hydroxide types adsorbed to the negative side of sulphide on the pyrite surface by chargeless iron hydroxide-cation complexes (Fuerstenau and Misra 1980; Fomasiero and Ralston, 1992). The results showed a remarkable change in the zeta potential values of galena and pyrite minerals particularly at pH 9 and at dosages of 50 g/Mg and 75 g/Mg SIBX. It has been confirmed that there is a strong interaction between the pyrite and galena mineral surfaces and SIBX.

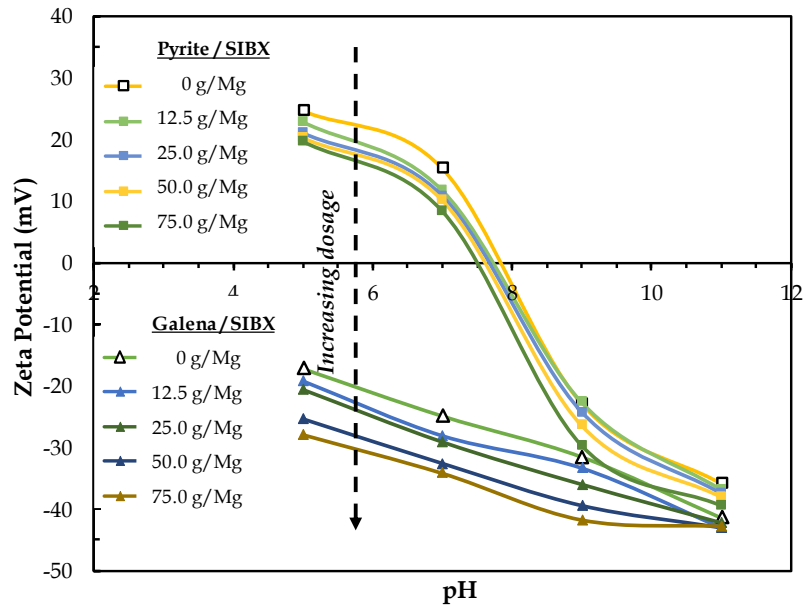Fig. 6. Results for pyrite and galena particles as a function of pH in the presence of different dosages of SIBX
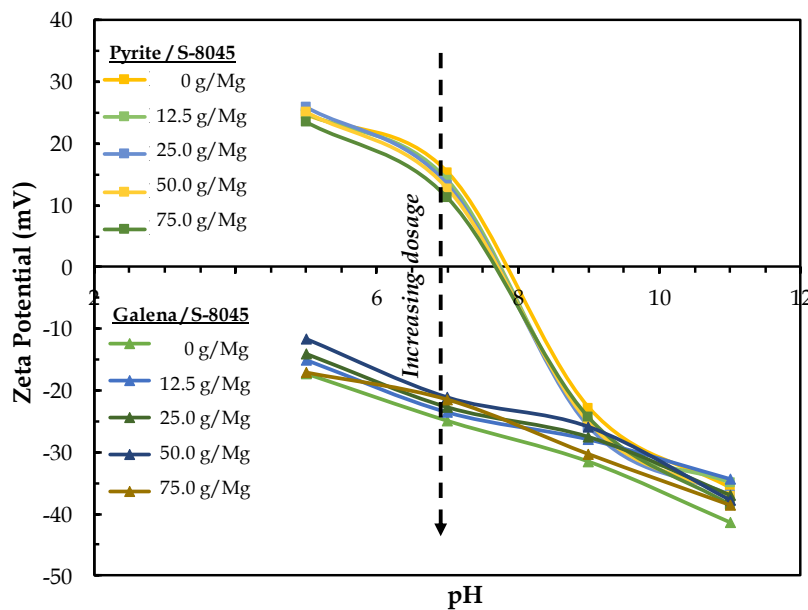

Fig. 7. Results for pyrite and galena particles as a function of pH in the presence of different dosages of S-8045

Lower surface adsorption was observed in all dosage values in studies conducted with S-8045 compared to SIBX (Fig. 7). The highest change in zeta potential was found to be -31.54 mV at pH 9 value.

Therefore, it was determined that the use of S-8045 as the sole collector in the flotation system might lead to a limited flotation performance. Compared to SIBX, it was observed that there was limited interaction between the pyrite/galena surfaces and S-8045 (thiophosphate) collector.

On the other hand, the zeta potential of pyrite/galena samples in the presence of MX-505 could not be measured due to the high amount of froth formation in Uzgiris cell as MX-505 has a 100% active surface and alcohol-based components.

3.3. Bubble-particle attachment time experiments

Figs. 8 and 9 show the bubble-particle attachment efficiencies for the galena and pyrite particles as a function of collector (S-8045, SIBX, and MX-505) dosage, respectively. As seen from Fig. 8a-c, the efficiencies increased with the increase of the collector dosage. The weakest interaction was observed with S-8045 at higher contact times in the presence of 12.5 g/Mg and 25 g/Mg with attachment time values below 50%. For the dosages of 50 g/Mg and 75 g/Mg, the attachment time values were above 50% at all contact times, and the bubble-particle attachment times (> 50% attachment time) were below 1 ms. SIBX showed attachment values above 50% in all doses and contact times. Especially in the dosages of 50 g/Mg and 75 g/Mg, the attachment values ranged from 95% to 100% in 1 ms contact time. MX-505 showed 100% attachment values in all doses and contact times.

Pyrite is defined as naturally hydrophobic only under special conditions (characteristics of sulfide, low oxygen content, inert atmosphere, and natural pH of 6.8) (Fuerstenau & Sabacky, 1981; Kocabag et al., 1990; Chen et al., 2014) because pyrite mineral surface is attracted to N_2 more than water (Zhao et al., 2014). In the present study, the pyrite sample showed hydrophilic behavior at natural pH 5 in pure water without any collector. The results for the bubble particle measurement for pyrite in the presence of Aero S-8045, SIBX, and MX-505 are given in Fig. 9a-c, respectively.

The weakest interaction was observed with S-8045 which had low attachment times at all collector dosages with the attachment time values below 50%. The highest attachment rate in the presence of S-8045 was reached at 75 g/Mg dosage approximately as %50 at 1000 ms contact time. The attachment rates in the presence of SIBX increased with the increase in the dosage. Especially in the dosages of 50 g/Mg and 75 g/Mg, the attachment values ranged above 50% in 100 ms contact time. Pyrite particles showed much less floatability than galena at all SIBX dosages and contact times. The increase in the attachment time indicates a strong interaction between SIBX and galena than S-8045. Similar to the results obtained with galena, a stronger interaction between the pyrite surface and air bubbles also occurred in the presence of MX-505 which had a 100% attachment time at all doses and contact times, indicating a very strong interaction between pyrite particles and air bubbles.

These results also agree with the low recovery values obtained in the micro-flotation experiments as seen in Fig. 10 where the correlation between the bubble–particle attachment time and flotation recovery for the galena and pyrite particles. These results were in agreement with the micro-flotation results as low BPAT values resulted in higher flotation recoveries both for the galena and pyrite minerals. It appeared from the results that the adsorption of collector molecules at the surface of galena and pyrite particles took place and provided sufficient hydrophobicity for the flotation of the particles. In the experiments conducted with all of the collectors under the same conditions, the galena particles floated better than pyrite, thanks to its natural hydrophobicity to a degree.

The images from the bubble particle attachment time experiments for the galena and pyrite particles carried out at collector dosages of 12.5 g/Mg for S-8045, SIBX, and MX-505 are shown in Fig. 11. As seen in Fig. 11, the amount of both galena and pyrite particles attached on the bubbles increased in the presence of from S-8045 to MX-505. While the use of S-8045 in galena minerals resulted in significantly lower attachment rates because S-8045 could not be effectively adsorbed on the surface of galena minerals. The attachment rate of particles increased with the use of SIBX and a high interaction with the galena surface was obtained with MX-505 as also observed in the large aggregates of galena particles attached to the bubble surfaces in the presence of MX-505. The reason for this can be attributed to the higher molecular length of the MX-505 and the adhesive tendency of S atoms to the mineral surface as also observed from the highest attachment rates with MX-505 for both galena and pyrite particles during the bubble-particle attachment experiments at the low contact times (1 and 10 ms). These also indicate a very strong interaction between galena particles and air bubbles.
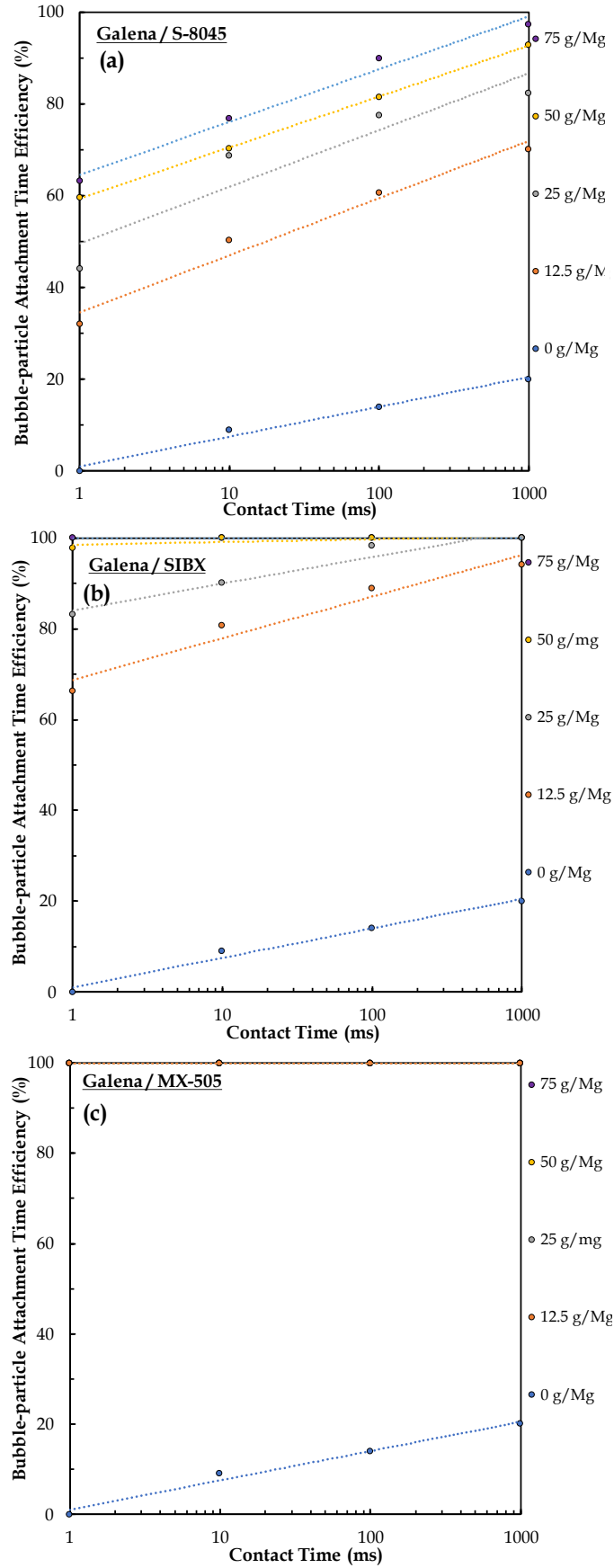
Fig. 8. Bubble-particle attachment efficiency for galena particles as a function of collector dosage (a) S-8045 (b) SIBX, and (c) MX-505
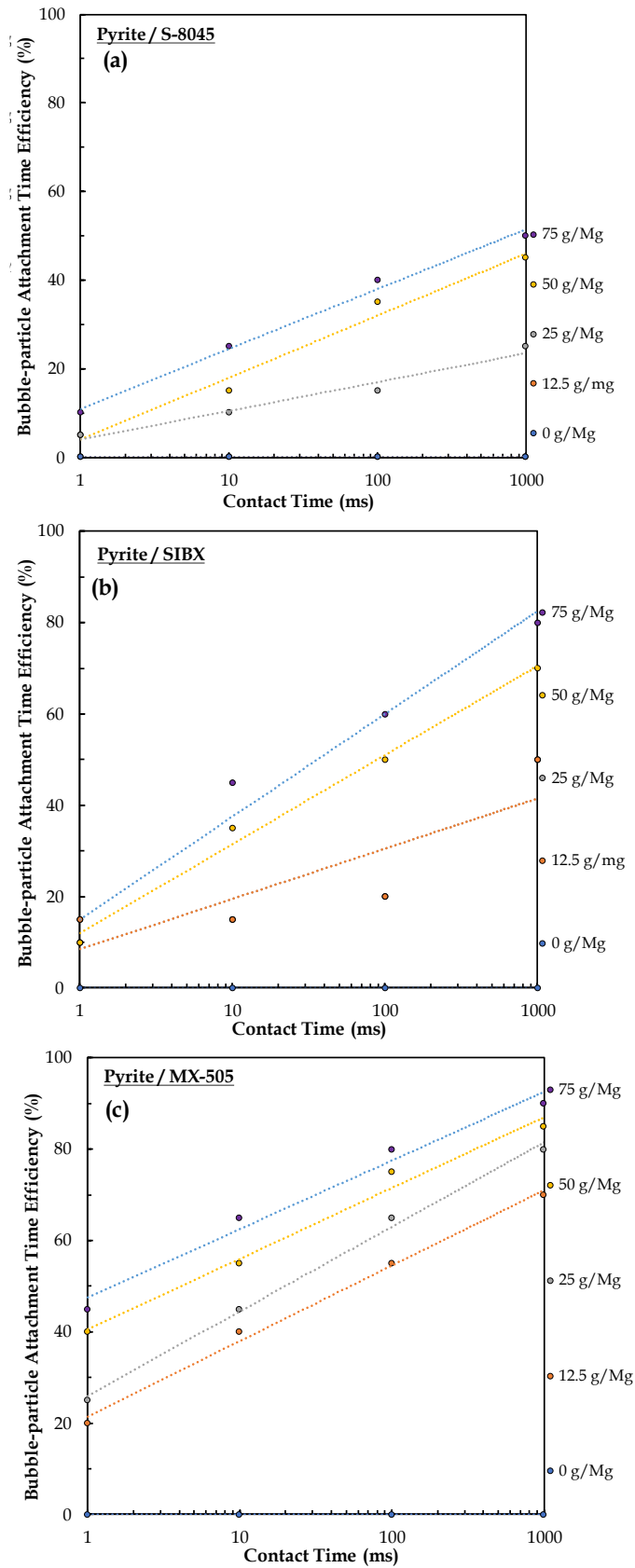
Fig. 9. Bubble-particle attachment efficiency for pyrite particles as a function of collector dosage (a) S-8045 (b) SIBX, and (c) MX-505
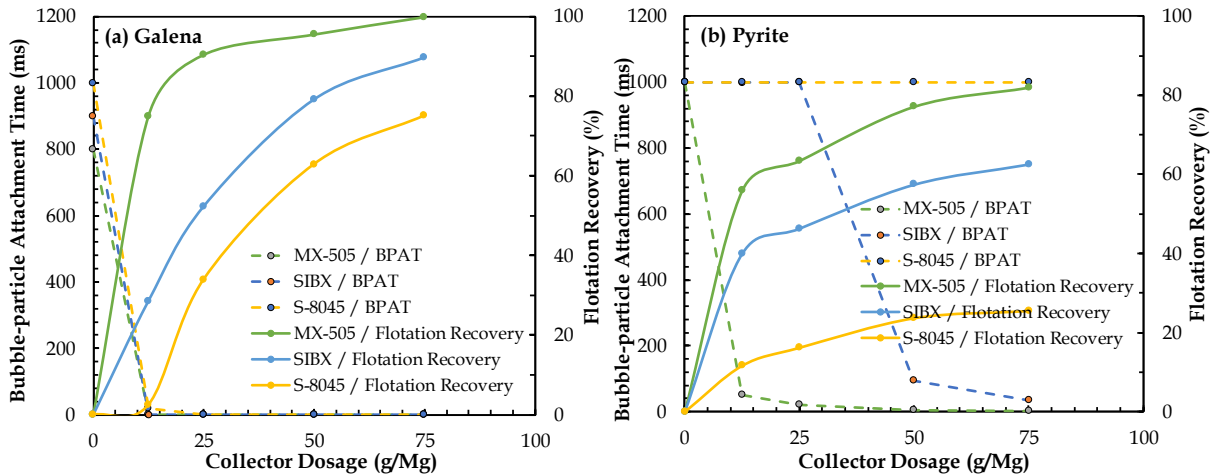
Fig. 10. Correlation between the bubble–particle attachment time and flotation recovery for the (a) galena and (b) pyrite particles as a function of collector dosages
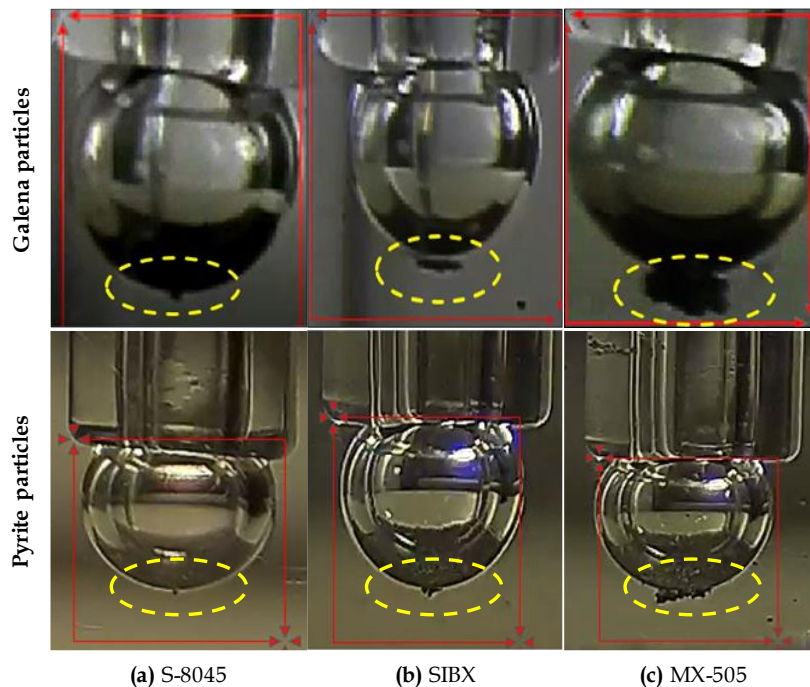

Fig 11. Bubble-galena and pyrite particle aggregates in the presence of (a) S-8045, (b) SIBX, and (c) MX-505 collectors (Bubble diameter = ~2 mm, contact time = 1 ms, collector dosage = 12.5 g/Mg)

Overall, the attachment performance of the particles to the air bubble is listed as the following in terms of not only the attachment rates but also the number of particles adhering to the air bubble in the experiments carried out with galena and pyrite particles:

$$S\text{-}8045 < SIBX < MX\text{-}505 \tag{1}$$

In sulfide mineral flotation, xanthates are typically used as the primary collectors, while dithiophosphate and carbamates serve as secondary collectors. However, the conventional use of these chemicals posed challenges due to their limited metal selectivity (Ackerman et al., 1987) Over the past two decades, extensive research has been conducted to enhance the selectivity of dithiophosphate and carbamates, resulting in increased selectivity and chelating through structural modifications and alterations (Liu et al., 2013). As a result, numerous chemicals with high selectivity and their blends are being successfully applied in industrial practices.

Chelating agents have acted an important role in improving the selectivity of collectors. It can be

categorized based on the donor atoms (N, O, P, or S) or the number of bonds to the metal for each chelating molecule. Donor atoms of the collectors used in experiments are shown as blue, red, orange, and yellow in Table 2. The atoms O and N exhibit an electron-withdrawing inductive effect. The chemical S-8045 consists of donor atoms P and S. The high electronegativity of the O atoms attached to the RO group in this chemical composition exert an electron-withdrawing effect. This effect leads to electron delocalization and stabilization of the anion. In the case of the xanthates, the P atom is more electropositive than the C atom. As a result of the decreased electron density of S in S-8045, it exhibits higher selectivity and weaker collecting properties compared to xanthates. This effect is less pronounced due to the lower number of RO groups in xanthates. The donor atoms in MX-505 are S, O, and N. S is a highly active donor and exhibits a strong binding tendency with S on the sulfide surfaces. N is less electronegative than O and has a high tendency to donate electrons. The electron density order among the donors in the composition is S > O > N, while the size and polarization order is S > N > O. Therefore, it can be said that the S atom in MX-505 might have a significant role in increasing selectivity by interacting with the S on the sulfide surface. Highly active nature of this structure making the MX-505 a potent collector. Additionally, N and O donors are also might be contributed to this enhanced strength. In conclusion, while the collector strength can be ranked as MX-505 > Xanthate > S-8045, selectivity follows the opposite order (Glembotskii, 1978; Somasundaran and Nagaraj, 1984).

Moreover, the reason for achieving higher efficiency in the galena mineral compared to the pyrite mineral in tests conducted with the MX-505 blend chemical containing thiocarbamate might also lie in the lower affinity of thiocarbamate compounds towards the Fe sites on the surface of pyrite (Mkhonto et al., 2022). Furthermore, higher flotation recoveries obtained with MX-505 for both minerals compared to the xanthate and dithiophosphate collectors can be attributed to the hydration layer on mineral surfaces can be effectively eliminated by IPETC, allowing it to subsequently adsorb onto active sites (Bu et al., 2018). Although it has been shown in the literature that thiocarbamate collectors are generally used for their selectivity against the pyrite, it is observed that this situation is associated with their high Cu site selectivity. It has also been observed that high pyrite flotation yields up to pH 10 can be obtained with thiocarbamates, which interact with Cu or Fe on the mineral surfaces, in the absence of Cu-containing surfaces in the environment (Forson et al., 2021).

The results obtained within this study have clearly shown that the limited natural floatability rates of galena and pyrite can be enhanced by chemicals derived from thiocarbamates with greater effectiveness compared to xanthate and thiophosphate.

4. Conclusions

This study aimed to investigate the flotation behaviour of galena and pyrite minerals in the presence of, xanthate-thiocarbamate-monothiophosphate collectors, namely Aero S-8045 (Thiophosphate), SIBX (Xanthate), and Aero float MX-505 (Thiocarbamate). For this purpose, the micro-flotation experiments of pure galena and pyrite particles with S-8045, SIBX, and MX-505 were conducted. Additionally, the zeta potential and bubble-particle attachment time experiments were carried out to explain the flotation efficiencies of the minerals. While higher flotation efficiencies for both minerals were obtained with MX-505, S-8045 gave the lowest flotation recovery. The zeta potential experiment of these minerals indicated that the galena mineral showed a negative charge at all studied pH values (5 to 11, no point of zero charge (pzc) was determined, and the pzc of pyrite was determined at pH≈8. In the case of the bubble-particle attachment experiments, while there was a considerable increase in the efficiencies in the case of S-8045, this effect was so significant in the case of MX-505 that 100% efficiency was obtained at all MX-505 dosages from 12.5 g/Mg to 75 g/Mg. This indicates that MX-505 is the strongest collector for the galena particles compared to others. Meanwhile, the same effect was observed for the pyrite particles the order from the highest to lowest was obtained from MX-505 and S-8045. However, this effect was not strong as pyrite particles in the presence of these collectors. Bubble-particle attachment observations were in agreement with micro-flotation results. An inverse relationship was observed between flotation efficiency and bubble-particle attachment times. In other words, low attachment times resulted in high flotation recoveries for both galena and pyrite. It can be concluded from this study that the chemical adsorption effectiveness from the point of view of recovery was determined to be in the following order: Thiocarbamates (MX-505) > Xanthate (SIBX) > Thiophosphates (S-8045).

As a future work, a detailed investigation of the molecular structure of blend chemicals, as well as the chelates formed on the pyrite and galena surfaces, in addition to surface-based chemical analyses such as XPS, FTIR, and AFM will contribute to a better understanding of the interaction between the collectors and the mineral surfaces. Furthermore, both laboratory batch, pilot-scale, and facility-scale tests are planned based on the results obtained in this study.

References

ACKERMAN P.K., HARRIS G.H., KLIMPEL R.R., APLAN F.F., 1987. *Evaluation of flotation collectors for copper sulfides and pyrite, I. Common sulfhydryl collectors*. International Journal of Mineral Processing, 21, 105-127.

ALBIJANIC, B., OZDEMIR, O., HAMPTON, M.A., NGUYEN, P.T., NGUYEN, A.V., BRADSHAW, D., 2014. *Fundamental aspects of bubble–particle attachment mechanism in flotation separation*, Minerals Engineering 65, 187–195.

ALBIJANIC, B., OZDEMIR, O., NGUYEN, A.V., BRADSHAW, D., 2010. *A review of induction and attachment times of wetting thin films between air bubbles and particles and its relevance in the separation of particles by flotation.* Advances in Colloid and Interface Science, 159 (1), 1–21.

ALBIJANIC, B., AMINI, E., WIGHTMAN, E., OZDEMIR, O., NGUYEN, BRADSHAW, D.J., 2011. *A relationship between the bubble–particle attachment time and the mineralogy of a copper–sulphide ore*. Minerals Engineering, 24, 1335–1339.

BAE, S., MANNAN, M.B., & LEE, W., 2012. *Adsorption of cationic cetylpyridinium chloride on pyrite surface.* Journal of Industrial and Engineering Chemistry, 18(4), 1482-1488.

BU, Y., HU, Y., SUN, W., GAO, Z., & LIU, R., 2018. *Fundamental flotation behaviors of chalcopyrite and galena using o-isopropyl-n-ethyl thionocarbamate as a collector*. Minerals, 8(3), 115.

BULATOVIC, S.M., 2007. *Handbook of flotation reagents: chemistry, theory and practice: Volume 1: flotation of sulfide ores*. Elsevier, 323-351.

CHEN, J., LONG, X., & CHEN, Y., 2014. *Comparison of multilayer water adsorption on the hydrophobic galena (PbS) and hydrophilic pyrite (FeS$_2$) surfaces: a DFT study.* The Journal of Physical Chemistry C, 118(22), 11657-11665.

CHEN, W., CHEN, F., ZHANG, Z., TIAN, X., BU, X., & FENG, Q., 2021. *Investigations on the depressant effect of sodium alginate on galena flotation in different sulfide ore collector systems*. Minerals Engineering, 160, 106705.

CONSUEGRA, G.L., KUTSCHKE, S., RUDOLPH, M., & POLLMANN, K., 2020. *Halophilic bacteria as potential pyrite bio-depressants in Cu-Mo bioflotation*. Minerals Engineering, 145, 106062.

CUI, W., ZHANG, J., & CHEN, J., 2021. *Surface proximity effect of galena and its influence on synergistic adsorption behavior*. Applied Surface Science, 567, 150847.

DELANY, B., 1940. *Flotation*. Industrial & Engineering Chemistry, 32(9), 1172-1173.

DONG, Z., JIANG, T., XU, B., LI, Q., ZHONG, H., & YANG, Y., 2021. *Selective flotation of galena using a novel collector S-benzyl-N-ethoxy carbonyl thiocarbamate: An experimental and theoretical investigation*. Journal of Molecular Liquids, 330, 115643.

ELIZONDO-ÁLVAREZ, M.A., FLORES-ÁLVAREZ, J.M., DÁVILA-PULIDO, G.I., & URIBE-SALAS, A., 2017. *Interaction mechanism between galena and calcium and sulfate ions*. Minerals Engineering, 111, 116-123.

ELIZONDO-ÁLVAREZ, M.A., DÁVILA-PULIDO, G.I., BELLO-TEODORO, S., & URIBE-SALAS, A., 2018. *Role of pH on the adsorption of xanthate and dithiophosphinate onto galena*. Canadian Metallurgical Quarterly, 58(1), 107-115.

FAIRTHORNE, G., FORNASIERO, D., & RALSTON, J., 1997. *Interaction of thionocarbamate and thiourea collectors with sulphide minerals: a flotation and adsorption study*. International Journal of Mineral Processing, 50(4), 227-242.

FENG, Q.C., WEN, S.M., BAI, X., CHANG, W.H., CUI, C.F., ZHAO, W.J., 2019. *Surface modification of smithsonite with ammonia to enhance the formation of sulfidation products and its response to flotation*. Minerals Engineering, 137, 1–9.

FINKELSTEIN, N.P., ALLISON, S.A., LOVELI, V.M. and STEWART, B.V., 1975. *Natural and induced hydrophobicity in sulfide mineral systems, in Advances in Interfacial Phenomena of Particulate: Solid/Gas Systems*. ed. P. Somasundaran and R.B. Grieves, Am. lost. Chem. Engrs., New York, 165-175.

FORNASIERO, D., & RALSTON, J., 1992. *Iron hydroxide complexes and their influence on the interaction between ethyl xanthate and pyrite*. Journal of Colloid and Interface Science, 151(1), 225-235.

FORSON, P., SKINNER, W., & ASAMOAH, R., 2021. *Decoupling pyrite and arsenopyrite in flotation using thionocarbamate collector*. Powder Technology, 385, 12-20.

FUERSTENAU, D.W., MISHRA, R.K., 1980. *On the mechanism of pyrite flotation with xanthate collectors. In: Jones, J.J. (Ed.), Complex Sulfide Ores*. The Institution of Mining and Metallurgy, London, pp. 271 – 278.

FUERSTENAU, M.C., & SABACKY, B.J., 1981. *On the natural floatability of sulfides*. International Journal of Mineral Processing, 8(1), 79-84.

GAUDIN, A.M., & MALOZEMOFF, P., 1932. *Recovery by flotation of mineral particles of colloidal size*. The Journal of Physical Chemistry, 37(5), 597-607.

GAUDIN, A.M., SCHUHMANN JR, R., & SCHLECHTEN, A.W., 1942. *Flotation kinetics. II. The effect of size on the behavior of galena particles*. The Journal of Physical Chemistry, 46(8), 902-910.

GAUDIN, A.M., MIAW, H.I. & SPEDDEN, H.R., 1957. *Native floatability and crystal structure.*, 2nd Int. Congr. of Surface Activity, vol: 2, S. FS 451.

GLEMBOTSKII, V.A., 1953. *The time of attachment of air bubbles to mineral particles in flotation and its measurement*. Izv. Akad. Nauk SSSR (OTN), No. 11: 1524-1531.

GLEMBOTSKII, V.A. KLASSEN, V.I. and PLAKSIN, I.N., 1963. *Flotation*, Primary Sources, N.Y., S.19.

GLEMBOTSKII, V.A., 1978. *Theoretical principles of forecasting and modifying collector properties*. Tsvet Metally, 51(2), 86.

GU, G., XU, Z., NANDAKUMAR, K., & MASLIYAH, J., 2003. *Effects of physical environment on induction time of air–bitumen attachment.* International Journal of Mineral Processing, 69(1-4), 235-250.

GUNGOREN, C., OZDEMIR, O., WANG, X., OZKAN, S.G., MILLER, J.D., 2019. *Effect of ultrasound on bubble-particle interaction in quartz-amine flotation system*. Ultrasonics Sonochemistry, 52, 446-454.

HERD, H.H., & URE, W., 1941. *Surface chemistry in the flotation of galena*. The Journal of Physical Chemistry, 45(1), 93-106.

HODOUIN, D., JAMSA-JOUNELA, S.L., CARVALHO, M.T., & BERGH, L., 2001. *State of the art and challenges in mineral processing control*. Control Engineering Practice, 9(9), 995-1005.

HUANG, X., HUANG, K., JIA, Y., WANG, S., CAO, Z., & ZHONG, H., 2019. *Investigating the selectivity of a xanthate derivative for the flotation separation of chalcopyrite from py*rite. Chemical Engineering Science, 205, 220-229.

HUANG, X., YUAN, X., YANG, H., ZHANG, R., LIU, G., & ZENG, J., 2023. *Evaluating the adsorption mechanism of a novel thiocarbamate on chalcopyrite and pyrite particles*. Advanced Powder Technology, 34(2), 103935.

IKUMAPAYI, F., MAKITALO, M., JOHANSSON, B., & RAO, K.H., 2012. *Recycling of process water in sulphide flotation: Effect of calcium and sulphate ions on flotation of galena*. Minerals Engineering, 39, 77-88.

JIANG, C.L., WANG, X.H., & PAREKH, B.K., 2000. *Effect of sodium oleate on inhibiting pyrite oxidation*. International Journal of Mineral Processing, 58(1-4), 305-318.

JIN, J., WANG, X., GAO, P., LIU, J., ZHU, Y., & HAN, Y., 2021. *Selective adsorption behavior and mechanism of a high-performance depressant in the flotation separation of pyrite from talcum*. Journal of Molecular Liquids, 325, 114707.

KOCABAG, D., 1983. *The oleophilicity/hydrophobicity of galena and pyrite in two-liquid flotation*. Ph.D. thesis, Mineral Resources Engineering, 52-55.

KOCABAG, D., SHERGOLD, H.L., & KELSALL, G.H., 1990. *Natural oleophilicity/hydrophobicity of sulphide minerals*. II. Pyrite. International Journal of Mineral Processing, 29(3-4), 211-219.

KOSMULSKI, M., 2009. *Surface charging and points of zero charge.* (Vol. 145). CRC press.

LONG, X., CHEN, Y., CHEN, J., XU, Z., LIU, Q., & DU, Z., 2016. *The effect of water molecules on the thiol collector interaction on the galena (PbS) and sphalerite (ZnS) surfaces: A DFT study*. Applied Surface Science, 389, 103-111.

LIU G.Y., XIAO J.J., ZHOU D.W., ZHONG, H., CHOI, P., XU, Z.H., 2013. *A DFT study on the structure-reactivity relationship of triphosphorous acids as flotation collectors with sulfide minerals: Implication of surface adsorption*. Colloids Surface A-Physicochemical Engineering Aspects, 434:243-252.

MCKEE, D.J., 1991. *Automatic flotation control-a review of 20 years of effort*. Minerals Engineering, 4(7-11), 653-666.

MCFADZEAN, B., CASTELYN, D.G., & O'CONNOR, C.T., 2012. *The effect of mixed thiol collectors on the flotation of galena*. Minerals Engineering, 36, 211-218.

MCFADZEAN, B., MHLANGA, S.S., & O'CONNOR, C.T., 2013. *The effect of thiol collector mixtures on the flotation of pyrite and galena*. Minerals Engineering, 50, 121-129.

MKHONTO, P.P., ZHANG, X., LU, L., XIONG, W., ZHU, Y., HAN, L., & NGOEPE, P.E., 2022. *Adsorption mechanisms and effects of thiocarbamate collectors in the separation of chalcopyrite from pyrite minerals: DFT and experimental studies*. Minerals Engineering, 176, 107318.

NAGARAJ, D.R., 1988. *The chemistry and application of chelating or complexing agents in minerals separations*. In Reagents in Mineral Technology, 257-334.

NAGARAJ, D.R., RAVISHANKAR, S.A., 2007. *Froth flotation: A century of innovation*. In: Fuerstenau, M.C., Jameson, G.J., Yoon, R.-H. (Eds.), Society for Mining, Metallurgy, and Exploration, Inc. (SME), pp. 375–424.

NGUYEN, A.V., 1994. *The collision between fine particles and single air bubbles in flotation*. Journal of Colloid Interface Science, 162(1): 123-128.

NGUYEN, A.V., SCHULZE, H.J., 2004. *Colloidal Science of Flotation*. CRC Press, Florida, USA.

NIKOLAEV, A.A., BATKHUYAG, A., & GORYACHEV, B.E., 2018. *Mineralization kinetics of air bubble in pyrite slurry under dynamic conditions*. Journal of Mining Science, 54(5), 840-844.

OZDEMIR, O., KARAKASHEV, S.I., NGUYEN, A.V., & MILLER, J.D., 2006. *Adsorption of carbonate and bicarbonate salts at the air–brine interface*. International Journal of Mineral Processing, 81(3), 149-158.

OZDEMIR, O., KARAGUZEL, C., NGUYEN, A.V., CELIK, M.S. and MILLER, J.D., 2009. *Contact angle and bubble attachment studies in the flotation of trona and other soluble carbonate salts*. Minerals Engineering, 22(2), 168-175.

OZDEMIR, O., TARAN, E., HAMPTON, M.A., KARAKASHEV, S.I., & NGUYEN, A.V., 2009. *Surface chemistry aspects of coal flotation in bore water.* International Journal of Mineral Processing, 92(3-4), 177-183.

OZUN, S., & ERGEN, G., 2019. *Determination of optimum parameters for flotation of galena: Effect of chain length and chain structure of xanthates on flotation recovery*. ACS omega, 4(1), 1516-1524.

OWUSU, C., E ABREU, S.B., SKINNER, W., ADDAI-MENSAH, J., & ZANIN, M., 2014. *The influence of pyrite content on the flotation of chalcopyrite/pyrite mixtures*. Minerals Engineering, 55, 87-95.

PARTRIDGE, A.C, SMITH G.W., 1971. Trans. Industry Mineral Metallurgy, C80, 199.

PECINA-TREVIÑO, E. T., URIBE-SALAS, A., NAVA-ALONSO, F., & PÉREZ-GARIBAY, R., 2003. *On the sodium-diisobutyl dithiophosphinate (Aerophine 3418A) interaction with activated and unactivated galena and pyrite*. International Journal of Mineral Processing, 71(1-4), 201-217.

QI, X., LI, X., LIANG, Y., WANG, H., GUO, W., CONG, X., & ZHANG, H., 2020. *Surface structure-dependent hydrophobicity/oleophilicity of pyrite and its influence on coal flotation*. Journal of Industrial and Engineering Chemistry, 87, 136-144.

SHEN, Y., NAGARAJ, D.R., FARINATO, R., & SOMASUNDARAN, P., 2016. *Study of xanthate decomposition in aqueous solutions*. Minerals Engineering, 93, 10-15.

SU, L., XU, Z., & MASLIYAH, J., 2006. *Role of oily bubbles in enhancing bitumen flotation*. Minerals Engineering, 19(6-8), 641-650.

SOMASUNDARAN, P., & NAGARAJ, D.R., 1984. *Chemistry and applications of chelating agents in flotation and flocculation*. Reagents in Mineral Industry, 209-219.

SWAINSON, S.J., & ANDERSON, A.E., 1931. *The promoter activity of alkyl xanthates*. Transactions of The Electrochemical Society, 60(1), 329.

VILINSKA, A., HANUMANTHA R.K., & FORSSBERG, K.E., 2007. *Selective coagulation in chalcopyrite/pyrite mineral system using Acidithiobacillus group bacteria*. Advanced Materials Research, 20, 366-370.

XING, Y., GUI, X., CAO, Y., 2017. *Effect of bubble size on bubble-particle attachment and film drainage kinetics – a theoretical study*. Powder Technology, 322, 140–146.

YE, Y. & MILLER, J.D., 1988. *Bubble/particle contact time in the analysis of coal flotation*. Coal Prep. (Gordon & Breach), 5(3-4): 147-166.

YOON, R.H. & YORDAN, J.L., 1991. *Induction time measurements for the quartz-amine flotation system*. Journal of Colloid and Interface Science, 141(2): 374-383.

ZHANG, W., SUN, W., HU, Y., CAO, J., & GAO, Z., 2019. *Selective flotation of pyrite from galena using chitosan with different molecular weights*. Minerals, 9(9), 549.

ZHAO, C.H., CHEN, J.H., WU, B.Z., & LONG, X.H., 2014. *Density functional theory study on natural hydrophobicity of sulfide surfaces*. Transactions of Nonferrous Metals Society of China, 24(2), 491-498.

ZHAO, W.J., LIU, D.W., FENG, Q.C., WEN, S.M., CHANG, W.H., 2019. *DFT insights into the electronic properties and adsorption mechanism of HS− on smithsonite (101) surface*. Minerals Engineering, 141 105846.